HISTORICAL TRENDS IN THE JET STREAMS

Cristina L. Archer and Ken Caldeira
Department of Global Ecology, Carnegie Institution of Washington, Stanford, CA 94025 (USA)

1.   INTRODUCTION

Jet streams are narrow bands of fast, meandering air currents that flow around the globe at the tropopause level in both hemispheres. They are often classified in two categories: sub-tropical jets, found at the poleward margin of the upper branch of the Hadley circulation, and polar jets, located above the polar-frontal zone, a region of sharp thermal contrast between cold polar air and warm tropical air (Holton 1992; Bluestein 1993). Jet streams are important because synoptic scale disturbances tend to form in the regions of maximum jet stream wind speed and to propagate downstream along storm tracks that follow the jet axes (Holton 1992). Changes in jet stream location, intensity, or altitude can therefore cause variations in frequency and intensity of storms. Also, jet streams inhibit formation and development of hurricanes, which preferentially develop in low-shear regions of the atmosphere (Gray 1968; Vecchi and Soden 2007). They affect air transport not only because of their high winds, but also because of the clear-air turbulence associated with jet cores (Bluestein 1993).

2.   DATA

To study whether jet streams have been changing in the past decades, we used two reanalyses of historical weather data: the ERA-40 (Uppala et al. 2005), from the European Centre for Medium-Range Weather Forecasts, which covers 1958 to 2001, and the NCEP/NCAR (Kalnay et al. 1996; Kistler et al. 1999), from the National Centers for Environmental Protection and the National Center for Atmospheric Research, covering 1948 to 2006. Monthly means of u- and v-wind components, together with temperature, were available at 2.5 degrees horizontal resolution and with 6 vertical levels between 400 and 100 hPa. Whereas conventional observations (e.g., upper-air winds, temperature, and humidity from radiosondes; surface data from various land and buoy networks; ocean wave heights) were assimilated in both datasets throughout the entire periods, satellite-borne observations (e.g., infrared and microwave radiances; total and column ozone; surface-pressure and winds over ocean) were only assimilated from 1979 on. For this reason, this study will only focus on the period 1979-2001. Despite limitations (Pawson and Fiorino 1999), the ERA-40 and NCEP/NCAR datasets are the best sets of reanalyzed weather data available (Uppala et al. 2005).

3.   METHODS

In both hemispheres, the jet streams are located between the 400 and the 100 hPa levels. The Northern Hemisphere (NH) jet has a single-band spiral-like structure, generally beginning south of the Canary Islands and ending one circumnavigation later over England. The southern hemisphere jet has a more concentric structure, with a persistent ring around Antarctica, hereafter referred to as Southern Hemisphere Polar (SHP) jet, and a seasonally varying second ring at about 30 S, hereafter referred to as the Southern Hemisphere sub-Tropical (SHT) jet (Koch et al. 2006). Jet streams are not continuous, but rather fragmented, meandering, and with notable wind speed and elevation variations. As such, the task of clearly identifying jet stream boundaries at a given time can be difficult and ambiguous (Koch et al. 2006).

To overcome this problem, we define jet stream properties via integrated quantities, which are more numerically stable and less grid-dependent than are simple maxima and minima. First, for each horizontal grid point in the reanalyses, we define the mass weighted average wind speed between 400 and 100 hPa (WS) as:

$$WS_{i,j} = \frac{\sum_{z=400mb}^{z=100mb} m_z \times \sqrt{u_{i,j,z}^2 + v_{i,j,z}^2}}{\sum_{z=400mb}^{z=100mb} m_z}, \qquad (1)$$

where z is the vertical coordinate, $u_{i,j,z}$ and $v_{i,j,z}$ are the monthly-mean horizontal wind components at grid point (i,j,z), and m_z is the mass at level z. Figure 1 shows the 1958-2001 average of WS, the mass weighted average wind speed, obtained from the ERA-40 dataset for all grid points (the pattern of WS from NCEP/NCAR is almost identical). The figure shows wind maxima to the East of the continents in the northern hemisphere, and to the East of Australia and to the South of Africa in the southern hemisphere, as observed (Koch et al. 2006). Note that jet streams are located at latitudes between 15 and 70 degrees (N and S). The zonal average of WS shows a single maximum in the northern hemisphere around 40 N, consistent with a single-band spiral-like structure, and two maxima in the southern hemisphere at 30 and 60 S, consistent with a two-ring structure.
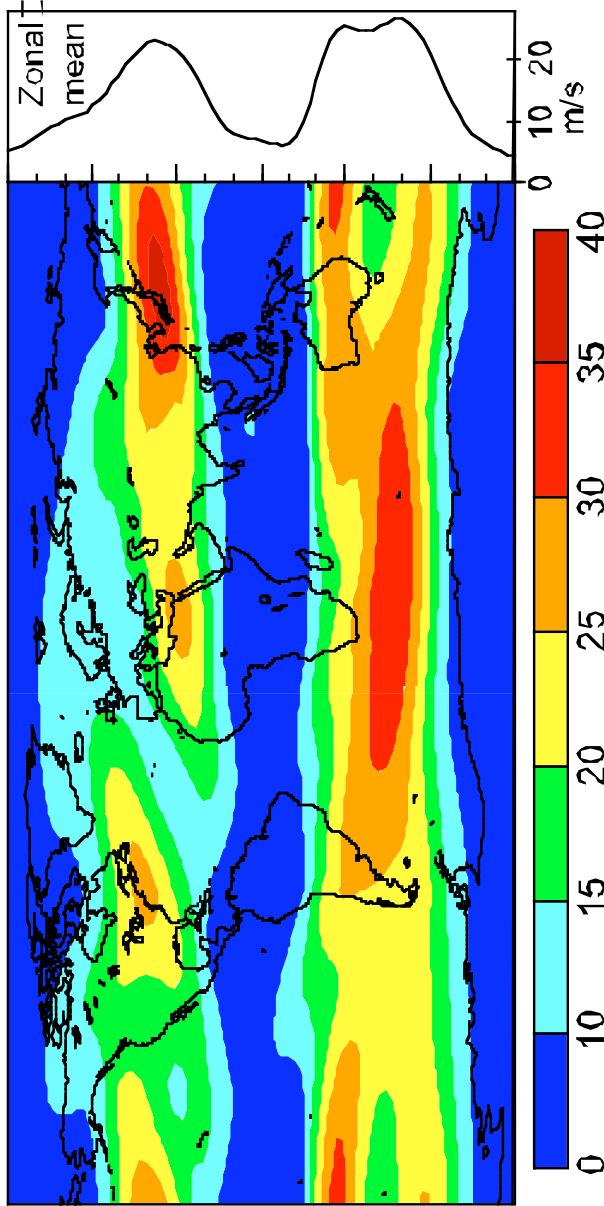
Figure 1   Average jet stream wind speed (m/s) from the ERA-40 dataset for the period 1979-2001, with the zonal average shown in the right panel.

Given mass and wind speed at each pressure level z between 400 and 100 hPa, for each horizontal grid cell, the mass-flux weighted pressure P is defined as:

$$P_{i,j} = \frac{\sum_{z=400mb}^{z=100mb}\left(m_z \times \sqrt{u_{i,j,z}^2 + v_{i,j,z}^2}\right) \times p_{i,j,z}}{\sum_{z=400mb}^{z=100mb} m_z \times \sqrt{u_{i,j,z}^2 + v_{i,j,z}^2}}. \quad (2)$$

P represents the average pressure of flows near the tropopause, and therefore the average altitude of these flows. Because jet streams are found at the tropopause, we can use P to characterize the height of both the jet streams and the tropopause. In both hemispheres, the average jet stream height decreases monotonically from the equator to the pole between 10 and 50 (N and S) from ~230 to ~260 hPa (not shown).

Given the total mass-flux between 400 and 100 hPa, we calculate the mass-flux weighted latitude in the Northern Hemisphere (L^{NH}) for each longitude i in the gridded reanalysis fields as follows:

$$L_i^{NH} = \frac{\sum_{j=15N}^{j=70N}\left[\sum_{z=400mb}^{z=100mb}\left(m_z \times \sqrt{u_{i,j,z}^2 + v_{i,j,z}^2}\right)\right] \times \varphi_j}{\sum_{j=15N}^{j=70N}\sum_{z=400mb}^{z=100mb} m_z \times \sqrt{u_{i,j,z}^2 + v_{i,j,z}^2}}, (3)$$

where ϕ_j is the latitude. We use this integrated value to characterize the latitude of the NH jet stream at each longitude i. Note that the NH jet is defined in equation (3) as latitudes between 15N and 70N. Similarly, the latitudes of the SHT and the SHP jets (L^{SHT} and L^{SHP}) are defined from equation (3) by setting the latitude bounds to 40S-15S and 70S-40S, respectively. These intervals were chosen based on the zonal mean in Figure 1. On average, the NH jet was farthest south (36 N) over North Africa and farthest north (40 N) over the North Atlantic; the latitude of the SHT jet varied between 30 and 27 S, whereas the SHP latitude varied between 54 and 50 S (not shown).

4.   RESULTS

Using these grid-cell and longitude-band jet stream properties, simple scalar metrics for the entire globe (or for regions of interest) can be obtained. We calculated global-average latitude, wind speed, and pressure of the three jet streams (NH, SHT, and SHP) for 23 years (1979-2001) from both the ERA-40 and the NCEP/NCAR datasets. The trends of yearly averages are shown in the next figures and the linear regression parameters are listed in Table 1. To correct for auto-correlation in the time-series, we applied the Zwiers and Storch (1995) test of statistical significance at the two-sided 10% significance level.

All three jet streams moved poleward during the period 1979-2001 (Figure 2), at rates varying from 0.06-0.11 degrees/decade in the SHT, to 0.07-0.10 degrees/decade in the SHP, and to 0.17-0.19 degrees/decade in the NH. A poleward shift of the jet streams is consistent with an expansion of the Hadley cell with increased mean temperature, as shown in idealized simulations by Frierson et al. (2007), who also found a smaller but similar widening of the Hadley cell with increased equator-to-pole temperature gradient. Also Mitas and Clement (2005) found a significant intensification of the NH winter Hadley cell in both the ERA-40 and the NCEP/NCAR reanalyses. The

connection of poleward expansion of the Hadley cell with global warming was identified by Lu et al. (2007), who found, in a strong green house gas emission scenario, an average expansion of 0.6 degrees/K, equivalent to a poleward shift of the jet streams by 0.05 degrees/decade, comparable to the values found in this study. Fu et al. (2006) estimated that the jet streams in both hemispheres shifted poleward by about 1 degree in 27 years, or 0.37 degrees/decade, equivalent to an expansion of the Hadley cell by 4 degrees/K, given a 0.5 K increase in global temperature over the same period (Lu et al. 2007).
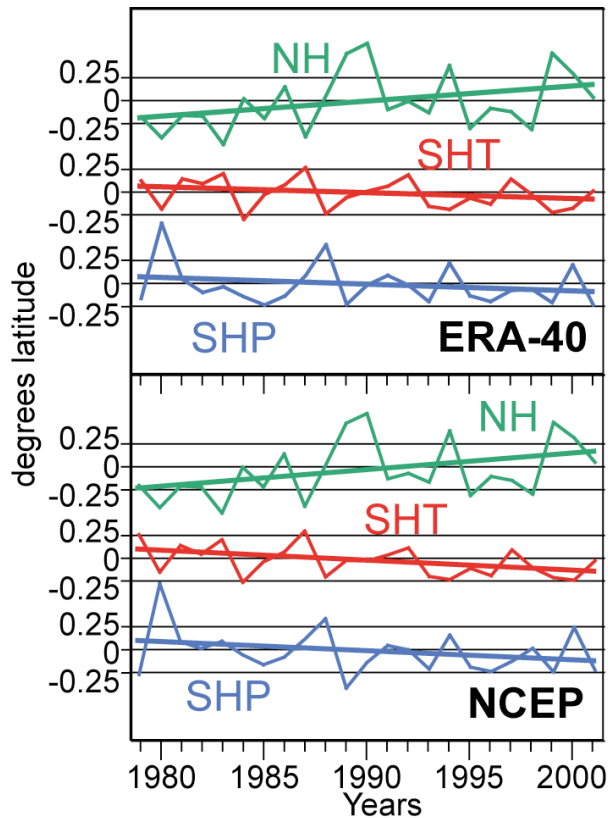

Figure 2   Anomalies from the 23-year (1979-2001) average latitudes of the jet streams from the ERA-40 (top) and the NCEP/NCAR (bottom) datasets.

An increase in jet stream altitude implies a negative change in pressure and is reflected in a negative pressure trend in Table 1 and Figure 3. In the ERA-40 dataset, all jet streams had negative and statistically significant pressure trends. In the NCEP/NCAR dataset, the NH and SHP jet streams had negative pressure trends, but the SHT showed no significant trend. Significant pressure decreases occurred in the SHP jet (-0.41 to -0.83 hPa/decade, or +10 to +22 m/decade). The NH jet showed a significant decrease in pressure in the ERA-40 dataset (-0.42 hPa/decade, or about +11 m/decade). These increases in jet stream altitude were 4 to 10 times less than those found for the global mean tropopause height by Santer

et al. (2003), who reported an average increase in tropopause altitude of ~95 m/decade for the 1979-1999 period.
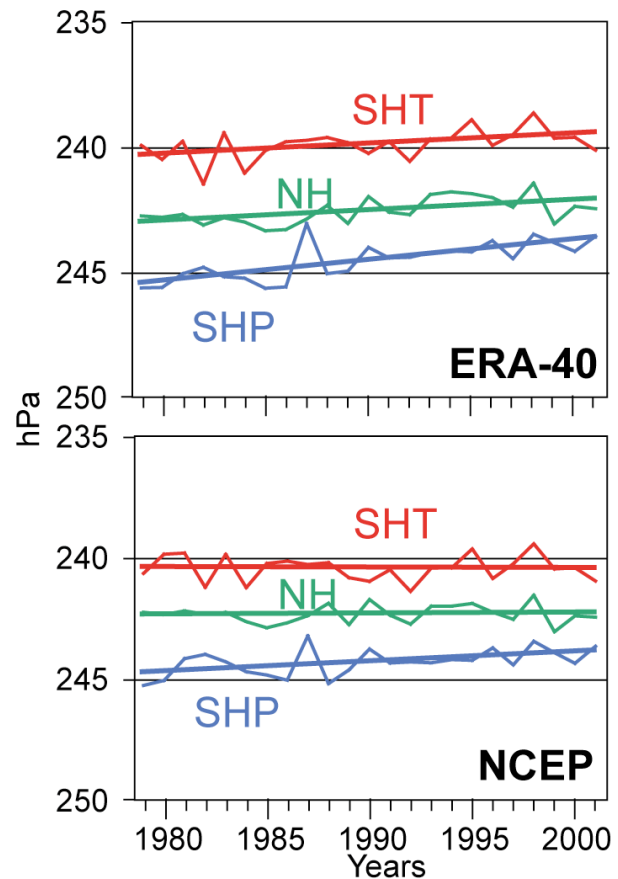

Figure 3   Pressure at the jet streams during 1979-2001 from the ERA-40 (top) and the NCEP/NCAR (bottom) datasets. Pressure increases correspond to lowerings of the jet streams, and vice versa.

The strength, or wind speed, of the jet streams decreased slightly in the NH jet (-0.15 to -0.18 m/s/decade), decreased in the SHT jet (-0.37 to -0.42 m/s/decade), and increased in the SHP jet (+0.27 to +0.39 m/s/decade), consistently in both datasets. The increasing trend in the SHP jet winds is consistent with findings by Russell et al. (2006), who reported an increase in the westerlies over the Southern Ocean of ~20% in the past 20 years, and by Thompson and Salomon (2002), who related these increases to photochemical ozone losses.
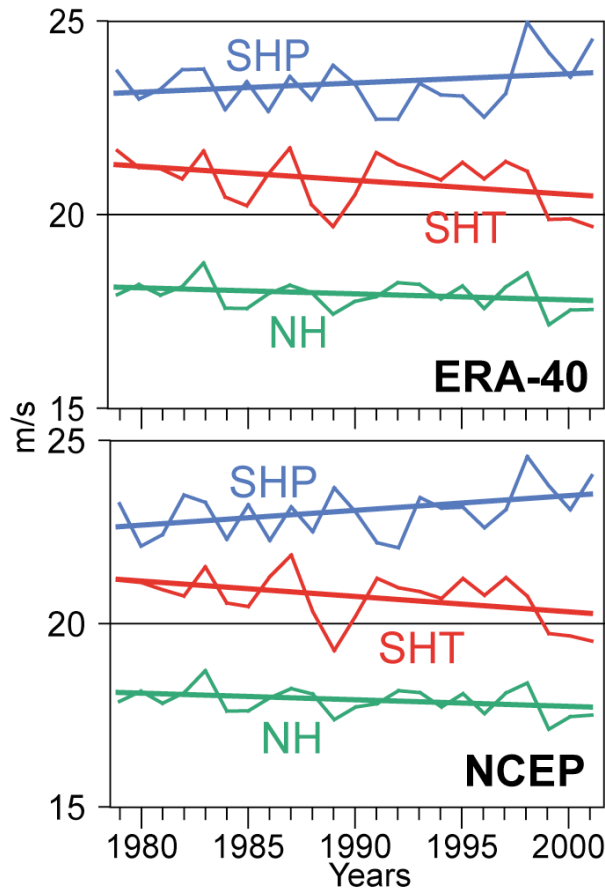
Figure 4   Jet stream wind speed (m/s) during 1979-2001 from the ERA-40 (top) and NCEP/NCAR (bottom) reanalyses.

In general, the two reanalyses ERA-40 and NCEP/NCAR showed a remarkably consistent behavior for the jet streams.

5.   INTERPRETATION

We calculated the jet stream zonal-average wind speeds and altitudes for each month during 1979-2001 from the ERA-40 and the NCEP/NCAR datasets and performed a linear regression analysis. The two reanalyses were again consistent with each other with respect to trends in jet stream wind speed (Figure 5). In the NH jet, an increase in wind speed north of 40N is more than compensated for by a decrease south of 40N, which confirms that the jet lost its strength. In the southern hemisphere, wind speed was generally decreasing in the sub-tropical jet (between 15 and 40S) and generally increasing in the polar jet (between 40 and 70S), as previously noted. Figure 5 also confirms that all jets shifted towards the poles, as positive trends of wind speed in the poleward edges of the jets were accompanied by negative trends in the equatorward edges.
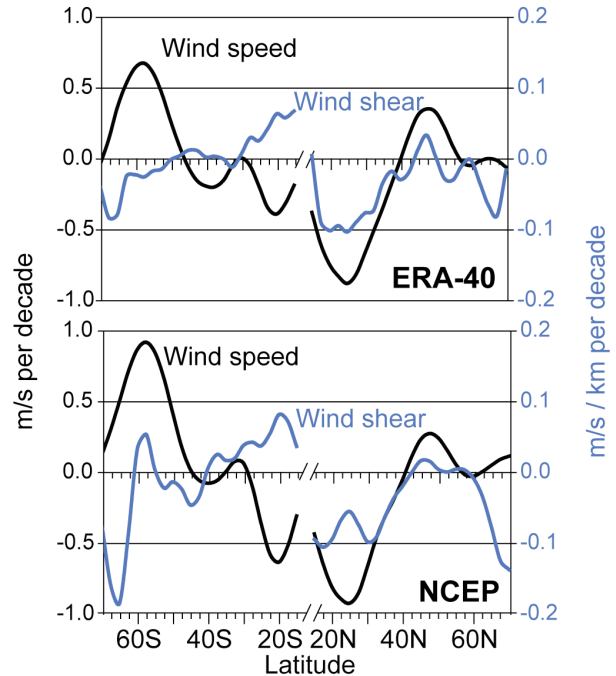

Figure 5   Slopes of the linear regression of monthly zonal-average wind speed and wind shear of the jet streams from the ERA-40 (top) and the NCEP/NCAR (bottom) reanalyses for the period 1979-2001.

From the thermal wind equation, wind shear of geostrophic flows (such as the jet streams) is related to the meridional temperature gradient as follows:

$$\frac{\partial u}{\partial z} = -\frac{g}{fT}\frac{\partial T}{\partial y} = -\frac{g}{fRT}\frac{\partial T}{\partial \varphi}, \tag{4}$$

where u is the west-east wind component, T is temperature, φ is latitude, f is the Coriolis parameter, g is gravity, and R the gas constant (Peixoto and Oort 1992). This equation suggests that the thermal structure of the troposphere can, to a first approximation, affect trends in jet stream wind speed. To further simplify the analysis, we used surface temperature in Eq. (4). Being a function of the meridional distance between grid cells, which is rather coarse in the reanalyses (2.5 degrees), zonal averages of wind shear from Eq. (4) are expected to be more irregular than those of jet stream wind speed.

Figure 5 shows slopes from the regression analysis of zonal wind shear from Eq. (4). In the NH jet, trends of thermal wind are correlated with trends in jet stream wind speed (r=0.49 in NCEP and 0.38 in ERA-40), which suggests that the meridional temperature gradients have been affecting the jets. In the southern hemisphere, conversely, trends of jet stream wind speed appear to be non-correlated (or even anti-correlated) with trends of thermal wind, which suggests that the thermal wind equation is too simplified an approach for the southern hemisphere jet streams.

The ERA-40 and NCEP datasets were not as consistent with respect to the altitude of the jet streams (Figure 6) as they were for wind speed. The ERA-40 pressure trends were negative everywhere, to indicate that the tropopause near the jet streams was rising in general. In the NCEP dataset, localized areas of lowered tropopause were found near 30 (N and S), 45N, and north of 65N in the NCEP reanalysis. Fu et al. (2006) suggested a localized rise in the troposphere at 30 N and S, in contrast to the decrease in the tropopause height that we found in the NCEP reanalysis fields at the same latitudes.

As surface temperatures rise because of global warming, the height of the tropopause is expected to increase (Santer et al. 2003). However, trends from a linear regression analysis in Figure 6 show that this simplified relationship between tropopause height and surface temperature does not necessarily hold for the jet streams (Figure 6). Although both reanalyses suggest overall negative (positive) trends in NH jet stream pressure (height) coexisting with warming trends in surface temperature, the latter are monotonic whereas the former have maxima and minima. In the southern hemisphere, surface temperature trends are nearly zero, whereas the tropopause height near the jets is rising south of 40S (and lowering around 30S in the NCEP/NCAR dataset).
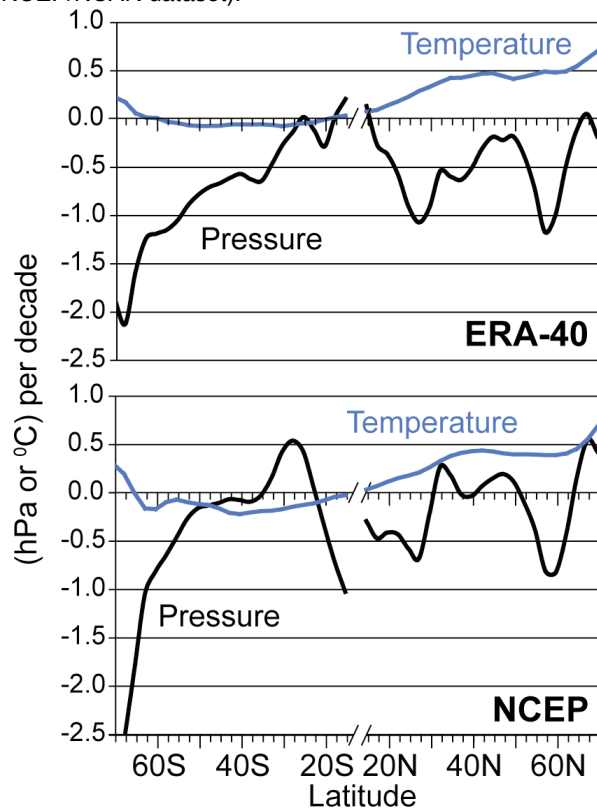

Figure 6   Trends of monthly zonal-average jet stream pressure and surface temperature from the

6.   CONCLUSIONS

Global warming is expected to affect the distribution of mass (and thus pressure) in the atmosphere and therefore affect the strength and location of the jet streams. We used the ERA-40 and the NCEP/NCAR reanalyses to study if and how the jet streams have changed in 1979-2001.

Trends in jet stream wind speed, altitude, and latitude, calculated via a technique based on mass and mass-flux averages, indicate that the jets are generally moving poleward and rising in both hemispheres. The northern hemisphere jet is weakening. In the southern hemisphere, the polar jet is strengthening, whereas the sub-tropical jet is weakening. These changes in jet stream latitude, altitude, and strength have the potential to affect the formation and evolution of storms in the mid-latitudes and of hurricanes in the sub-tropical regions, therefore impacting people in half of the globe.

Despite the complex nature of jet streams, which are discontinuous in time and space, meandering, and with notable wind speed and elevation variations, we tried to explain their changes with simple relationships. Variations of the equator-to-pole temperature gradients are expected to affect the jet stream wind speed and latitude via the thermal wind equation. We found that this approach gives satisfactory results to explain wind speed trends in the northern hemisphere jet, but not in the southern. Increased greenhouse gas concentrations are expected to warm and raise the tropopause near the jet streams. Although we found that this was true in general, we could not explain the details of the observed trends in jet stream height by simply looking at surface temperature trends.

7.   REFERENCES

Arguez, A., H. J. Diamond, F. Fetterer, A. Horvitz, and J. M. Levy, 2007: State of the climate in 2006. Special supplement to the *Bull. Am. Meteorol. Soc.*, **88***,* 135 pp.

Bluestein, H. B., 1993: *Synoptic-dynamic meteorology in midlatitudes. Volume II: Observations and theory of weather systems*. Oxford University Press, 594 pp.

Frierson, D. M. W., J. Lu, and G. Chen, 2007: Width of the Hadley cell in simple and comprehensive general circulation models. *Geophys. Res. Lett.*, **34**, L18804, doi:10.1029/2007GL031115.

Fu, Q., C. M. Johanson, J. M. Wallace, and T. Reichler, 2006: Enhanced mid-latitude tropospheric warming in satellite measurements. *Science,* **312**, 1179, doi:10.1126/science.1125566.

Holton, J. R., 1992: *An introduction to dynamic meteorology*, Academic Press, 511 pp.

Kalnay, E., M. Kanamitsu, R. Kistler, W. Collins, D. Deaven, L. Gandin, M. Iredell, S. Saha, G. White, J. Woollen, Y. Zhu, M. Chelliah, W. Ebisuzaki, W. Higgins, J. Janowiak, K.C. Mo, C. Ropelewski, J. Wang, A. Leetmaa, R. Reynolds, R. Jenne, and D. Joseph (1996), The NCEP/NCAR 40-year reanalysis project. *Bull. Amer. Meteor. Soc.*, **77**, 437-471.

Kistler, R., E. Kalnay, W. Collins, S. Saha, G. White, J. Woollen, M. Chelliah, W. Ebisuzaki, M. Kanamitsu, V. Kousky, H. van den Dool, R. Jenne, and M. Fiorino, 1999: The NCEP-NCAR 50-Year Reanalysis. *Bull. Amer. Meteor. Soc.*, **82**, 247-267.

Koch, P., H. Weirnli, and H. C. Davies, 2006: An event-based jet-stream climatology and typology. *Int. J. Climatol.,* **26**, 283-301, doi:10.1002/joc.1255.

Lu, J., G. A. Vecchi, and T. Reichler, 2007: Expansion of the Hadley cell under global warming. *Geophys. Res. Lett.*, **34**, L06805, doi:10.129/2006GL028443.

Mitas, C. M., and A. Clement, 2005: Has the Hadley cell been strengthening in the recent decades? *Geophys. Res. Lett.*, **32**, L03809, doi:10.129/2004GL021765.

Pawson, S., and M. Fiorino, 1999: A comparison of reanalyses in the tropical stratosphere. Part 3: inclusion of the pre-satellite data era. *Clim. Dynam.*, **15**, 241-250.

Peixoto, J. P. and A. H. Oort, 1992: *Physics of climate*. American Institute of Physics. 520 pp.

Russell, J. L., K. W. Dixon, A. Gnanadesikan, R. J. Stouffer, and J. R. Toggweiler, 2006: The southern hemisphere westerlies in a warming world: propping open the door to the deep ocean. *J. Climate*, **19**, 6382-6390.

Santer, B. D., M. F. Wehner, T. M. L. Wigley, R. Sausen, G. A. Meehl, K. E. Taylor, C. Ammann, J. Arblaster, W. M. Washington, J. S. Boyle, W. Brüggemann, 2003: Contributions of anthropogenic and natural forcing to recent tropopause height changes. *Science,* **301**, 479-483, doi: 10.1126/science.1084123.

Schubert, S. D., M. J. Suarez, P. J. Pegion, R. D. Koster, and J. T. Bacmeister, 2004: Causes of long-term drought in the U.S. Great Plains. *J. Climate*, **17**, 485-503.

Thompson, D. W. J., and S. Salomon, 2002: Interpretation of recent southern hemisphere climate change. *Science*, **296**, 895-899.

Uppala, S.M., Kållberg, P.W., Simmons, A.J., Andrae, U., da Costa Bechtold, V., Fiorino, M., Gibson, J.K., Haseler, J., Hernandez, A., Kelly, G.A., Li, X., Onogi, K., Saarinen, S., Sokka, N., Allan, R.P., Andersson, E., Arpe, K., Balmaseda, M.A., Beljaars, A.C.M., van de Berg, L., Bidlot, J., Bormann, N., Caires, S., Chevallier, F., Dethof, A., Dragosavac, M., Fisher, M., Fuentes, M., Hagemann, S., Hólm, E., Hoskins, B.J., Isaksen, L., Janssen, P.A.E.M., Jenne, R., McNally, A.P., Mahfouf, J.-F., Morcrette, J.-J., Rayner, N.A., Saunders, R.W., Simon, P., Sterl, A., Trenberth, K.E., Untch, A., Vasiljevic, D., Viterbo, P., and Woollen, J., 2005: The ERA-40 re-analysis. *Quart. J. R. Meteorol. Soc.*, **131**, 2961-3012, doi:10.1256/qj.04.176.

Vecchi, G. A., and B. J. Soden, 2007: Increased tropical Atlantic wind shear in model projections of global warming. *Geophys. Res. Lett.,* **34**, L08702, doi:10.1029/2006GL028905.

Zwiers, F. W., and H. Von Storch, 1995: Taking serial correlation into account in tests of the mean. *J. Climate*, **8**, 336-351.

Table 1 Statistical regression analysis for each jet stream (NH = Northern Hemisphere between 15 and 70N, SHT = Southern Hemisphere sub-Tropical between 15 and 40S, SHP = Southern Hemisphere Polar between 40 and 70S) and for each parameter (latitude, altitude, and wind speed) from both the ERA-40 and the NCEP/NCAR datasets for the period 1979-2001. Bold values indicate trends that are significant at the 10% significance level (two-sided) with the Zwiers-Storch test.

Parameter	Jet Stream	Dataset	Slope (per decade)	Intercept	Correlation coefficient (r)	P-value
Latitude (degrees)	NH	ERA-40	0.165	5.4	0.363	0.089
		NCEP	0.185	1.3	0.399	0.059
	SHT	ERA-40	-0.063	-15.5	-0.268	0.216
		NCEP	**-0.111**	**-6.0**	**-0.279**	**0.033**
	SHP	ERA-40	-0.073	-37.9	-0.428	0.309
		NCEP	-0.101	-32.3	-0.279	0.197
Pressure (hPa)	NH	**ERA-40**	**-0.419**	**326.0**	**-0.251**	**0.007**
		NCEP	-0.036	249.7	-0.066	0.766
	SHT	**ERA-40**	**-0.412**	**321.9**	**-0.076**	**0.028**
		NCEP	0.017	237.1	0.022	0.920
	SHP	**ERA-40**	**-0.832**	**410.1**	**-0.746**	**<0.001**
		NCEP	**-0.410**	**326.0**	**-0.506**	**0.014**
Wind Speed (m/s)	NH	ERA-40	-0.156	48.9	-0.287	0.185
		NCEP	-0.182	54.0	-0.337	0.116
	SHT	ERA-40	-0.365	93.5	-0.381	0.073
		NCEP	-0.422	104.7	-0.429	0.041
	SHP	ERA-40	0.237	-23.9	0.251	0.247
		NCEP	0.404	-57.3	0.420	0.046